Clinical Nuclear Medicine

SECOND EDITION

Clinical Nuclear Medicine

SECOND EDITION

Edited by

M. N. Maisey
Guy's Hospital
London

K. E. Britton
St Bartholomew's Hospital
London

D. L. Gilday
The Hospital for Sick Children
Toronto

CHAPMAN & HALL MEDICAL
London · New York · Tokyo · Melbourne · Madras

UK	Chapman & Hall, 2–6 Boundary Row, London SE1 8HN
JAPAN	Chapman & Hall Japan, Thomson Publishing Japan, Hirakawacho Nemoto Building, 7F, 1-7-11 Hirakawa-cho, Chiyoda-Ku, Tokyo 102
AUSTRALIA	Chapman & Hall Australia, Thomas Nelson Australia, 102 Dodds Street, South Melbourne, Victoria 3205
INDIA	Chapman & Hall India, R. Seshadri, 32 Second Main Road, CIT East, Madras 600 035

First edition 1983
Second edition 1991

Typeset in 9½/11½ Palatino by
Rowland Phototypesetting Ltd
Bury St Edmunds, Suffolk
Printed in Great Britain at the
University Press, Cambridge

ISBN 0 412 27900 2

British Library Cataloguing in Publication Data
Clinical nuclear medicine.
I. Nuclear medicine
I. Maisey, M. N. (Michael Norman) II. Britton, K. E. (Keith Eric) III. Gilday, D. L. (David L.)
616.07575

ISBN 0 412 27900 2

Contributors

D. Ackery, MB, MSc
Department of Nuclear Medicine
Southampton General Hospital
Southampton, UK

J. Ash, MD
Department of Nuclear Medicine
The Hospital for Sick Children
Toronto
Ontario, Canada

D. A. Brennand-Roper, MA, MRCP
Department of Cardiology
West Hill Hospital
Dartford
Kent, UK

A. B. Brill, MD, PhD
Department of Nuclear Medicine
University of Massachusetts Medical Center
Worcester
Massachusetts, USA

K. E. Britton, MD, MSc, FRCP
Department of Nuclear Medicine
St Bartholomew's Hospital
London, UK

S. E. M. Clarke, MBBS, MRCP, MSc
Department of Nuclear Medicine
Guy's Hospital
London, UK

A. J. Coakley, MSc, FRCP
Consultant in Nuclear Medicine
Department of Nuclear Medicine
Kent and Canterbury Hospital
Canterbury
Kent, UK

D. N. Croft, MA, DM, FRCP, FRCR
Department of Nuclear Medicine
St Thomas' Hospital
London, UK

P. J. Ell, MD, MSc, PD, MRCP, FRCR
Institute of Nuclear Medicine
University College and Middlesex Hospital Medical School
London, UK

A. T. Elliott, BA, PhD
Department of Clinical Physics and Bioengineering
Western Infirmary
Glasgow, UK

A. J. Fischman, MD, PhD
Division of Nuclear Medicine
Massachusetts General Hospital
Boston
Maryland, USA

I. Fogelman, MD, FRCP
Department of Nuclear Medicine
Guy's Hospital
London, UK

D. L. Gilday, BEng, MD, FRCP (C)
The Hospital for Sick Children
Toronto
Ontario, Canada

M. Granowska, MD, MSc
Department of Nuclear Medicine
St Bartholomew's Hospital
London, UK

N. D. Greyson, MD, FRCP (C)
Department of Nuclear Medicine
St Michael's Hospital
Toronto
Ontario, Canada

M. D. Gross, MD
Department of Internal Medicine
University of Michigan and Veteran's Administration Medical Center
Ann Arbor
Michigan, USA

A. J. W. Hilson, MB, MSc, MRCP
Department of Nuclear Medicine
Royal Free Hospital
London, UK

S. Howle, MD
The Hospital for Sick Children
Toronto
Ontario, Canada

J. Hutton, BSc, BPhil
Centre for Health Economics
University of York
York, UK

R. F. Jewkes, MB, FRCP
Department of Nuclear Medicine
Charing Cross Hospital
London, UK

F. A. Khafagi, MB BS, FRACP
Division of Nuclear Medicine
Department of Internal Medicine
University of Michigan
Ann Arbor
Michigan, USA

C. Lazarus, B Pharm, PhD, MPS
Department of Nuclear Medicine
Guy's Hospital
London, UK

S. M. Lewis, FRCPath
Department of Haematology
Royal Postgraduate Medical School
Hammersmith
London, UK

M. N. Maisey, MD, FRCP, FRCR
Department of Nuclear Medicine
Division of Radiological Sciences
Guy's Hospital
London, UK

N. J. Marshall, PhD
Department of Chemical Pathology
University College Hospital
London, UK

B. J. McNeil, MD
Department of Radiology
Harvard Medical School
Cambridge
Massachusetts, USA

R. Mistry
Department of Nuclear Medicine
Guy's Hospital
London, UK

A. M. Noyek, MD, FRCPC
Radiology Department
University of Toronto
Faculty of Medicine
Ontario, Canada

A. M. Peters, MD, MRCPath, MSc
Department of Diagnostic Radiology
Royal Postgraduate Medical School
Hammersmith
London, UK

M. Prentice, MD, MRCP
Department of Chemical Pathology
University College Hospital
London, UK

H. D. Royal, MD
Harvard Medical School
Cambridge
Massachusetts, USA

R. H. Secker-Walker, MD, MRCP
Division of Health Sciences
University of Vermont
Vermont, USA

B. Shapiro, MB ChB, PhD
Division of Nuclear Medicine
University of Michigan Medical Center
Ann Arbor
Michigan, USA

A. Sheldrake
Department of Chemical Pathology
University College Hospital
London, UK

P. Shepherd, MB, BS, MRCP
Department of Immunology
Guy's Hospital
London, UK

H. W. Strauss, MD
Division of Nuclear Medicine
Massachusetts General Hospital
Boston
Massachusetts, USA

N. Tamaki, MD
Division of Nuclear Medicine
Massachusetts General Hospital
Boston
Massachusetts, USA

H. N. Wagner, Jr, MD
Division of Nuclear Medicine
The Johns Hopkins Medical Institutions
Baltimore
Maryland, USA

P. Wells, BSC, MSc
Department of Medical Physics
Kent and Canterbury Hospital
Canterbury
Kent, UK

J. C. Williams, MA, MSc, FRCP
School of Postgraduate Studies in Medical and Healthcare
University College of Swansea
Swansea, UK

Preface to the first edition

Nuclear medicine is the bridge between a particular clinical problem and a relevant test using radionuclides. It began as a minor technical tool used in a few branches of medicine, notably endocrinology and nephrology. However, throughout the world it has now become established as a clinical discipline in its own right, with specific training programmes, special skills and a particular approach to patient management. Although the practising nuclear medicine physician must necessarily learn a great deal of basic science and technology, a sound medical training and a clinical approach to the subject remains of fundamental importance. It is for this reason that we have attempted in this book to approach the subject from a clinical standpoint, including where necessary relevant physiological material.

There exist many excellent texts which cover the basic science and technology of nuclear medicine. We have, therefore, severely limited our coverage of these aspects of the subject to matters which we felt to be essential, particularly those which have been less well covered in other texts – for example, the contents of Chapter 20 on Measurement by Royal and McNeill. Similarly, we have limited details of methodology to skeletal summaries of protocol (Appendix 1) and have included at the end of some chapters descriptions of particular techniques where we and the authors felt that it would be helpful. In order to emphasize the clinical approach of this book we have inverted the traditional sequence of material in chapters, presenting the clinical problems first in each instance. For similar reasons we have placed the chapters on Radiopharmaceuticals and Practical Instrumentation towards the end of the book.

Since medicine concerns the investigation, care and management of sick people who have specific problems, the virtues of a problem-orientated approach to the subject are becoming more widely recognized, particularly in the education of undergraduates. This approach has therefore been adopted in each chapter, making the overall structure of the book closer to that of a conventional textbook of medicine rather than a scientific treatise.

The contributors to this book come from both the United Kingdom and North America. As editors, in addition to requiring that authors should be expert in their field, we also wanted them to be particularly concerned about the day to day care of patients. We have endeavoured to emphasize the problem-orientated approach to clinical situations, whilst providing textual uniformity, without at the same time reducing the essentially individual contributions of each author.

We hope this textbook will be of value to a wide variety of medical professionals, including nuclear medicine clinicians in training, radiologists and clinicians from other specialities who use nuclear medicine in some form or other and require to know how it can help in solving their clinical problems. Finally, believing that medical students prefer the style of a textbook of medicine rather than that of a textbook of physics, we hope that the clinical priorities which have dictated the production of this book will encourage them to consult it.

M.N.M., K.E.B., London
D.L.G., Toronto

Preface to the second edition

Although adaptability and evolution are the key to growth, in medicine growth of a specialty is not an end in itself unless it contributes positively to patient care. Nuclear medicine is adapting to the changes in medicine and evolving to meet new challenges in a way which will ensure the discipline an important role in clinical medicine during this decade. Since the first edition of this textbook was published in 1984, significant changes have taken place in the way we practice our specialty. These changes have resulted from the development of new radiopharmaceuticals (^{99m}Tc-Sesta MIBI, ^{99m}Tc-HMPAO, ^{99m}Tc-MAG3 etc.), the development of improved instrumentation, new clinical applications for established radionuclide imaging methods and a wider appreciation and understanding of its benefits.

We believe that nuclear medicine is concerned with the way that the application of its investigative techniques to clinical problems can assist patient management and ultimately benefit patient outcome. We hope this is again reflected in this new edition. First the clinical problem is identified and this initiates the nuclear medicine investigation or treatment, whose pathophysiological role is explained and evaluated.

There are new areas of development in the speciality which we expect to have a clinical impact and which are likely to be incorporated into clinical practice during the lifetime of this edition. These have been included; in particular single photon and positron emission topography, immunoscintigraphy, single photon receptor imaging and new approaches to unsealed radioactive source therapy.

The practice of nuclear medicine is well established, but continuously changing. We hope that this edition will go some way towards consolidating the developments of the second half of the 1980s, provide some guidance to those of the early 1990s and even some pointers to the 21st century.

M.N.M., K.E.B., London
D.L.G., Toronto

Contents

CHAPTER ONE

Radionuclide imaging of the heart

N. Tamaki, A. J. Fischman and H. William Strauss

1.1 INTRODUCTION

Approximately 43 million Americans have one or more forms of acquired heart or blood vessel disease: high blood pressure occurs in 38 million adults; coronary artery disease occurs in 4.5 million adults; rheumatic heart disease occurs in 2 million; and stroke in 1.9 million. Myocardial infarction caused approximately 555 000 deaths (25% of all mortality) in 1982. Some aspect of the pathophysiology of each of these diseases can be evaluated with radionuclide techniques. The disorders involving the heart produce the following abnormalities which can be evaluated with radionuclide techniques: (a) myocardial ischaemia (a reversible condition, caused by a temporary deficiency in the supply of oxygen to the myocardium due to atherosclerotic narrowing of the vessel); (b) myocardial infarction (an irreversible condition leading to death of a portion of the myocardium, most commonly caused by acute thrombotic coronary occlusion superimposed on pre-existing severe coronary atherosclerotic narrowing); and (c) cardiomyopathy (a category of diseases of unknown cause associated with either thickening of the myocardium (hypertrophic or infiltrative myopathy) or thinning of the muscle resulting in altered function).

Radionuclide studies of the heart and circulation are amongst the oldest uses of radioactive tracers in human subjects. In the mid-1920s, Herrmann Blumgart and his associate Soma Weiss embarked on a number of experiments to measure the velocity of blood in man (Blumgart and Weiss, 1927). To make these measurements 'non-invasively', they injected **radium C** into the vein of one arm and identified the arrival of the tracer by observing a cloud chamber (described a few years earlier by Wilson *et al.*) placed over an artery of the other arm.

Following the Second World War, the increased availability of radioisotopes for medical use and the introduction of sophisticated radiation detection instruments gave cardiovascular nuclear medicine the impetus for rapid growth. Prinzmetal *et al.* used the Geiger counter and radioiodinated albumin in 1948 to record the radiocardiogram, a technique for measuring right and left heart transit times and cardiopulmonary blood volume. Ten years later Rejali *et al.* (1958) described the first *in vivo* imaging procedure in cardiovascular nuclear medicine: the blood pool scan for the detection of pericardial effusion. In the early 1960s, rapid advances were made. In a three-year period from 1962 to 1965 the concepts of myocardial perfusion imaging, acute myocardial infarct imaging, fatty acid imaging and radionuclide angiocardiography were described. Over the next two decades these procedures were refined, improved, and found to be of significant value in the management of patients with heart diseases. Now, both single-photon and positron approaches are available for the evaluation of cardiac function, perfusion and metabolism as described in the following sections:

1. Anatomy and physiology
2. Blood pool imaging
   - (a) Equilibrium studies
     - (i) Radiopharmaceutical
     - (ii) Planar image recording
     - (iii) Analysis
   - (b) First-pass imaging
     - (i) Injection technique
     - (ii) Analysis
   - (c) Clinical applications
     - (i) Diagnosis and evaluation of coronary artery disease
     - (ii) Acute infarction
     - (iii) Aneurysm
     - (iv) Right ventricular abnormalities in infarction

(v) Prognosis
(vi) Cor pulmonale
(vii) Valvular disease
(viii) Cardiomyopathy
(ix) Pericardial effusion
(d) Tomography
(e) Non-imaging probe
3. Perfusion imaging
(i) Coronary injection
(ii) Intravenous injection
(iii) Characteristics of thallium
(iv) Data recording
(v) Interpretation
(vi) Dipyridamole
(vii) Sensitivity and specificity
(a) Clinical applications
4. Infarct avid imaging
(i) Non-specific agents for imaging myocardial necrosis
(ii) ^{99m}Tc-labelled pyrophosphate
(iii) Antimyosin
5. New radiopharmaceuticals
6. Positron emission tomography

1.2 ANATOMY

The adult heart weighs about 300 g and holds approximately 500 ml of blood. The heart is located in the lower portion of the thoracic cavity between the lungs. It is covered by a clear fibrous sac, the pericardium. The pericardium contains a minimal amount of fluid to act as a lubricant between the moving surface of myocardium and the other structures in the chest.

The atria serve as temporary reservoirs of blood returned to the heart. The atria are separated by a thin muscular wall, the atrial septum, while the ventricles are separated by the thicker, muscular, interventricular septum.

The right side of the heart receives venous blood (pO_2 about 40 mmHg) returning via the superior and inferior venae cavae to the right atrium. The blood traverses the tricuspid valve and enters the pyramid-shaped right ventricle. The right ventricle expels blood through the pulmonic valve into the pulmonary artery and lungs. Blood returns from the lungs (pO_2 about 100 mmHg) via the four pulmonary veins to the left atrium. The blood traverses the mitral valve, and enters the left ventricle. The left ventricle expels blood through the aortic valve into the aorta.

The myocardium receives its oxygen supply from the right and left coronary arteries. The left coronary artery divides into two main branches: the left anterior descending artery and left circumflex artery. The left anterior descending artery branches to supply the interventricular septum and anterolateral wall of the left ventricle. The left circumflex artery supplies the left atrium and posterior and lateral ventricular walls of the left ventricle. The right coronary artery supplies the right atrium, right ventricle and the inferior wall of the left ventricle. The true posterior wall of the left ventricle is supplied by the posterior descending coronary artery which is most commonly a branch of the right coronary artery, but may arise from the left circumflex (10%). Blood drains from the myocardium to the coronary veins which terminate in the coronary sinus of the right atrium.

1.3 PHYSIOLOGY

1.3.1 CIRCULATION

Deoxygenated venous blood, transporting carbon dioxide and metabolic waste products, flows from the tissues towards the heart via the veins. Although venous pressure is low, resistance to blood flow is also low, and blood flows through the large veins at 40 cm s^{-1} on its way to emptying into the right atrium at a pressure of <5 mmHg. Blood is expelled from the right ventricle at a pressure of 25 mmHg into the lungs. In the enormous capillary bed of the lungs, the velocity of blood slows to 1 mm s^{-1}, carbon dioxide is eliminated and oxygen is taken up. The oxygenated blood returns to the heart at a pressure of <5 mmHg. The left ventricle provides sufficient kinetic energy in the form of a systolic pressure of 120 mmHg, and flow rate of 50 cm s^{-1}, to permit the blood to travel to the furthest capillary bed and return to the heart. As in the pulmonary capillaries, the velocity of blood slows at the tissue capillaries, to permit the exchange of nutrients for waste products.

The valves in the heart prevent backflow. The blood is forced forward with such force that the tricuspid and mitral valves are anchored by muscle strands – chordae tendinae – into the ventricular walls to prevent the valve leaflets from prolapsing into the atria.

Starting in early diastole, the atria and ventricles are relaxed. Atrial pressure is slightly higher than ventricular pressure, the tricuspid

and mitral valves are open and blood passes from the atria to the ventricles. The aortic and pulmonary valves are closed, preventing backflow of blood. The majority (80–90%) of ventricular filling takes place in this passive fashion. Atrial contraction serves to 'top off' the ventricles with the last 10–20% of blood volume. The quantity of blood in the ventricle at the end of diastole (following atrial contraction) is called the end-diastolic volume (about 150 ml).

Ventricular systole starts as the myofibrils shorten and ventricular pressure rises. The initial rise in pressure causes the tricuspid and mitral valves to close. As the myofibrils continue to shorten, pressure in the ventricles rises at a rapid rate. The interval following atrioventricular (AV) valve closure, but prior to the generation of sufficient pressure to open the pulmonary and aortic valves, is the interval of isovolumetric contraction. Continued shortening of the myofibrils causes the ventricular pressure to exceed pulmonary and aortic pressure; the pulmonary and aortic valves open and ventricular ejection begins. During the 250–300 ms interval when the myofibrils shorten to their minimal length (ventricular systole), approximately one-half to two-thirds of the end-diastolic volume is ejected. The fraction of the end-diastolic blood volume ejected during the systolic interval is called the **ejection fraction** (normal values by blood pool imaging range from 50% to 65%). Blood returning to the left heart during the interval of ventricular ejection, when the tricuspid and mitral valves are closed, is stored in the atria. As a result, both the atrial volumes and pressures rise slightly during the interval of ventricular ejection. At the conclusion of ventricular ejection ventricular pressure falls rapidly, the pulmonary and aortic valves close, the ventricle continues to relax with no change in volume (isovolumetric diastole) until the interventricular pressure drops below the pressure in the atria and the tricuspid and mitral valves open, to commence the filling phase. At resting heart rates, filling occurs rapidly for the first half of diastole, as atrial pressure and volume decrease. The slow filling phase follows, with atrial systole contributing 15–20% of the stroke volume. At high heart rates, the slow filling phase disappears, and the atrial contribution is reduced.

A normal 70 kg adult has a stroke volume of 80–100 ml $beat^{-1}$; at a heart rate of 60–70 beats min^{-1} this provides a cardiac output of 5–7 l min^{-1}. The cardiac output is distributed to the organs in proportion to their oxygen requirements, which change from rest to exertion. The usual distribution of cardiac output at rest and during exercise is listed in Table 1.1.

1.3.2 HEART BEAT

The myocardium has an intrinsic rhythm of contraction. The sinoatrial (SA) node, a small mass of specialized cells embedded in the right atrium near the entrance of the superior vena cava (SVC), has the fastest inherent rhythm and supersedes other similar sites in the heart. As a result, the SA node usually serves as the impulse generator for the remainder of the heart. To coordinate contraction the myocardium has a conducting system, consisting of specific muscle fibres which carry an electrical message from the SA node through the AV node to the ventricles. The wave of depolarization begins in the SA node and spreads to the surrounding atrial myocardial fibres. There are no specialized conduction fibres in the atria, but the wave of excitation spreads from cell to cell and covers the atria within 0.08 s. Atrial systole requires approximately 0.1 s. To permit the completion of mechanical atrial systole and effect maximal ventricular filling, the electrical signal enters the AV node, where it is held, prior to spreading over the surface of the ventricles via the specialized conducting system. The rapid conduction along the His–Purkinje system and the left and right bundle branches and their ramifications causes depolarization of all the right and left ventricular cells to occur almost simultaneously.

Abnormalities of conduction are quite common and may have substantial effects on radionuclide studies of ventricular function (see below).

Table 1.1

	Fraction of cardiac output	
Organ	*Rest (5 l min^{-1})*	*Exercise (17.5 l min^{-1})*
Brain	15%	4%
Heart	4%	5%
Kidneys	20%	3%
Liver	10%	<2%
GI tract	15%	<1%
Skeletal muscle	20%	70%
Skin	6%	10%
Other	10%	5%

After McArdle *et al.* (1981).

1.4 BLOOD POOL IMAGING

Blood pool imaging comprises a series of radionuclide techniques to determine global and regional ventricular function. Four measurements can be made from these scans: (1) the ejection fraction (EF) – i.e. the amount of blood ejected each beat (stroke volume) divided by the amount of blood in the ventricle at the end of diastole (end-diastolic volume) – is the single most important indicator of global ventricular performance; (2) the motion of the walls of the left and right ventricles; (3) the relative size of the chambers (end-diastolic volumes); and (4) rates of filling and emptying of the ventricles.

Ventricular function can be measured either during the initial passage of radiopharmaceutical through the heart (first pass), or following equilibration of the tracer in the blood pool (equilibrium-gated blood pool imaging). The two approaches differ in the radiopharmaceuticals, techniques of data recording and data analysis. The values obtained for ejection fraction, however, are comparable. The equilibrium method averages information from several hundred cardiac cycles to produce a high count density image, which permits detection of subtle wall motion abnormalities. The first-pass approach is better suited to recording cardiac function under circumstances of rapid change. Overall, both methods provide an accurate assessment of cardiac chamber size and global function.

1.4.1 EQUILIBRIUM-GATED BLOOD POOL IMAGING

(a) Radiopharmaceutical

Equilibrium imaging requires a radiopharmaceutical that is retained within the blood pool such as ^{99m}Tc-labelled human serum albumin or autologous red blood cells. The former is available as a multi-dose kit radiopharmaceutical, while the latter is prepared for each patient. Red cells may be labelled either *in vitro* (Smith and Richards, 1976) *in vivo* (Pavel *et al.*, 1977), or by a modified *in vivo* approach (Callahan *et al.*, 1982).

The *in vivo* method involves the injection of approximately 1 mg of stannous ion (usually in the form of stannous pyrophosphate) intravenously to prime the red cells, followed at 20–30 min by 550–750 MBq (15–20 mCi) of ^{99m}Tc-pertechnetate to label the erythrocytes.

The modified *in vivo* approach provides a higher labelling efficiency than the *in vivo* method, without the usual requirement for centrifugation of the cells in the *in vitro* methods. The modified *in vivo* method involves the injection of approximately 1 mg of stannous ion (usually in the form of stannous pyrophosphate) intravenously to prime the red cells, followed at 20–30 min by withdrawal of 3–5 ml of whole blood into a heparinized, shielded syringe containing 550–750 MBq (15–20 mCi) of ^{99m}Tc-pertechnetate to label the erythrocytes. The cells are allowed to incubate at room temperature in the syringe for 10–15 min prior to reinjection.

The labelling efficiencies of the *in vitro* and *in vivo* methods are both over 90% (Hamilton and Alderson, 1977).

(b) Data collection

Frame mode The R wave of the patient's electrocardiograph (ECG) is usually employed as the physiological trigger. Following an R wave, images are recorded for a preset time/frame, usually 10–50 ms, until the next R wave occurs. The time/frame should be selected to permit the average cardiac cycle to fill all frames (e.g. to record a 16-frame gated scan in a patient with a heart rate of 60, a time/frame of 1000/16 = 62.5 ms should be employed). Relatively few counts (<5000) are recorded in each frame during a single cycle. At the time of the next R wave, the information from the first portion of this cardiac cycle is added to that from the previous cycle, the second portion is added in phase, etc. The process is repeated each time the triggering signal is received and information input into the appropriate set of computer frames or files over a period of about 10 min until a series of composite pictures is accumulated, each comprising the data from a sufficient number of cardiac cycles to record 200 000–400 000 counts per frame (usually 500–1000 beats). This method of data accumulation is referred to as 'frame mode' acquisition (Figure 1.1).

To ensure that the gated blood pool data will be an accurate representation of cardiac function the patient's condition must be stable during acquisition. To optimize the likelihood of detecting small wall motion abnormalities, pixel size in the computer should be <5 mm. The computer should be able to acquire the data with sufficient temporal resolution (<50 ms per frame at a heart rate of 80, <25 ms per frame at a heart rate of 160) that permits accurate calculation of the ejection frac-

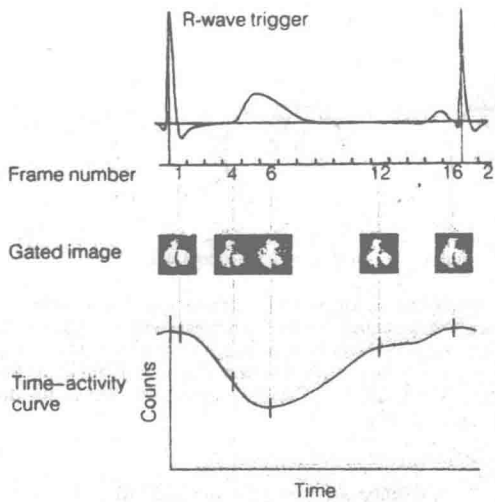

Figure 1.1 Diagram of 'frame mode' collection of a multigated scan. Selected images from a scan in a normal patient, recorded in the left anterior oblique position, are shown in the middle panel. The electrocardiogram (ECG) is shown in the top panel, and the time–activity curve derived from analysis of the blood pool images is shown in the bottom panel. The end-diastolic (ED) and end-systolic (ES) frames are marked.

tion (to compute filling rates the time/frame must be halved).

List mode When atrial fibrillation, marked sinus arrhythmia or multiple ectopic beats occur the R–R interval will vary. The data collected from short beats is terminated by the arrival of another R wave before the last few frames receive data. This results in terminal frames that contain fewer counts than the early frames with consequent degradation of the image quality. This may be partly overcome by computer rejection of short cycles or by setting the R–R interval for the computer at a time equal to the shortest beats. These approaches improve the visual quality of the images but do not permit accurate calculation of filling phase parameters because beats of different rates are averaged. Another method of dealing with the problem of an irregular heart rate is to acquire the study in 'list mode'. In list mode acquisition, the computer records the position of each photon recorded by the camera in sequence. When the acquisition is complete, this sequential list of data can be sorted by beat length, or the relationship of one beat to another. In addition, the data can be formatted either forward (from end-diastole through systole to the next diastole) or backwards (from end-diastole back through the previous systole). Backward-formatted data on beats of selected lengths provide a better assessment of the filling phase of the cardiac cycle than forward formatted data (Bonow *et al.*, 1981).

(c) Image recording

Rest A general all-purpose collimator with a regular or large field of view gamma camera provides an acceptable trade-off between sensitivity and resolution. After injection of the radiopharmaceutical, the patient is placed supine on the imaging table. Gated images are usually acquired in three views: (1) anterior; (2) left anterior oblique (LAO; optimized to best define the septum and maximize separation of the right and left ventricles); and (3) either the left lateral or left posterior oblique view (Figure 1.2). The left posterior oblique view is particularly useful for visualizing the inferobasal region of the left ventricle and the left atrium. Three views are necessary to visualize wall motion at the base, apex, septal and posterior walls of the left ventricle.

Exercise Left ventricular functional reserve can be measured by recording the blood pool scan during exercise. Since the duration of exercise is limited, data are usually recorded only in the LAO view during stress, to permit calculation of the changes in ejection fraction from rest to stress.

The patient should arrive in the laboratory in the fasted state, wearing light clothing, prepared for physical exertion. To minimize patient motion during physical exertion, the patient pedals a bicycle ergometer equipped with shoulder restraints and hand grips in either the supine or semi-supine position. Data are recorded for the last 2 min of each 3 min stage of exercise. The limited time for data collection usually requires a change from the all-purpose to a high-sensitivity collimator (a sensitivity improvement of a factor of two). The ECG and blood pressure are monitored throughout the procedure. Prior to exercise, images are obtained in both the anterior and LAO projections as described above. Exercise is started at 25 or 50 W and increased by regular increments of 25 W at 3 min intervals. The usual end points for the exercise test are:

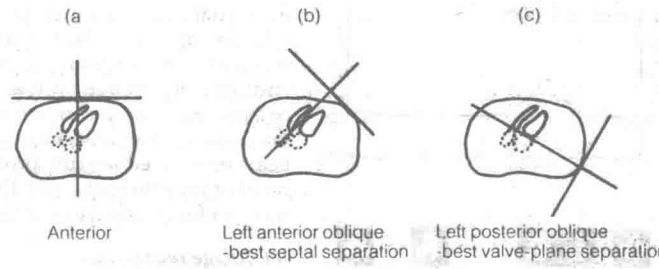

Figure 1.2 Diagram of positions employed for data collection in typical blood pool images. (a) The anterior view is recorded with the collimator of the scintillation camera just touching the anterior chest, with the patient in the supine position. (b) The left anterior oblique view is recorded with the patient in the supine position by rotating the detector to a position perpendicular to the axis of the septum (indicated by the dotted line). (c) The left posterior oblique view is recorded with the collimator parallel to the long axis of the left ventricle (indicated by the dotted line), with the patient rotated into the right lateral decubitus position.

1. severe angina pectoris;
2. hypotension;
3. significant arrhythmias;
4. severe fatigue;
5. achievement of 85% of predicted maximal heart rate.

Alternative approaches to large muscle dynamic exercise, such as isometric exercise (hand-grip) or immersion of the hand in ice-cold water ('cold pressor' test) are not as useful as large muscle dynamic exercise: isometric exercise may alter preload (via the Valsalva manoeuvre), and the cold pressor response may invoke reflexes which can depress cardiac function independent of ischaemia. As a result, large muscle dynamic leg exercise remains the method of choice for evaluating the functional reserve of the heart.

(d) Analysis

Gated blood pool scans are analysed in two parts: inspection of the data while they are displayed as an endless cinematic loop of the cardiac cycle, and quantification of volumes and function.

From inspection of the cinematic display the size of the chambers and great vessels is determined, regional wall motion is assessed, thickness of the muscular wall is estimated, and evidence is sought for pericardial effusion, spaces or masses. Normal subjects empty at least half the end-diastolic volume of their right and left ventricles each beat (normal left ventricular ejection fraction (LVEF) ranges from 50% to 65%); shorten the long axis of their left ventricle by >25% and the short axis by >45%; and have left ventricular end-diastolic volumes of <200 ml (114 ml m^{-2}). Inspection permits the subjective grading of regional wall motion into normal (regional shortening of a radius of at least 25%), hypokinetic (regional shortening of a radius of 10–25%), akinetic (regional shortening of 0–5%) and dyskinetic (systolic expansion), based on a comparison of end-diastolic to end-systolic outlines (Figure 1.3). When multiple images are recorded, or previous studies are compared to a new examination, the images should be examined side by side in simultaneous display to assess changes in cardiac size or regional wall motion.

Ejection fraction The ejection fraction (EF) is usually calculated by measuring the stroke counts and the background-corrected end-diastolic counts from regions of interest placed over the left ventricular blood pool data recorded in the LAO view (Parker *et al.*, 1972; Burow *et al.*, 1977) (Figure 1.1).

When the data are collected using the R wave for synchronization, the first frame of the collection corresponds to end-diastole. End-systole, the nadir of the curve, usually occurs between one-third and half-way through the series of images.

Prior to calculation of the EF, the counts in each frame of the data collection should be normalized, and a spatial and temporal smoothing of the data should be performed. A background region, located at about 3–6 o'clock from the left ventricle, free of branches of the pulmonary artery, left atrium and spleen, is selected, and the counts/

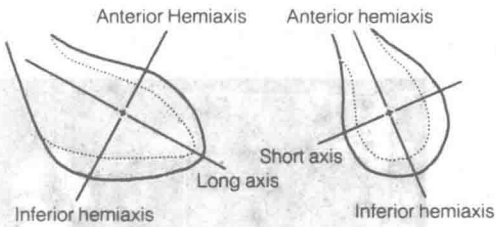

Figure 1.3 Diagram of end-diastolic outline (solid line) and end-systolic outline (dashed line) in (a) anterior view and (b) left anterior oblique view. The long and short axes are indicated by the heavy lines. Normal shortening is 50% of a radius in the short axes of the anterolateral, inferior and posterior walls. The septum should move posteriorly and thicken, but radial shortening may be limited to <15%.

picture element in the lung determined. A typical value for lung background is between 30% and 60% of left ventricular end-diastolic counts (depending on the radiopharmaceutical, window setting and collimator). This value is then subtracted from each picture element in the image. The background subtraction step is crucial to the subsequent calculation of the correct EF. Subtraction of too much background will result in a falsely elevated EF, while subtraction of too little background will result in a falsely depressed EF. The region of the left ventricle is then identified to the computer, and using either a manual, threshold or second derivative algorithm the edges of the left ventricle are identified on each frame. The total background-corrected counts in the left ventricle on each frame are used to generate the time–activity curve. The EF is calculated from the time–activity curve. In addition to the EF the time of filling, emptying, and ejection and filling rates can be readily computed from these curves. Filling and emptying rates of the left ventricle, important indexes of diastolic and systolic performance (Bonow *et al.*, 1981), are calculated from the time–activity curve by measuring either the average or peak slope of the desired phase.

An alternative approach to the calculation of EF uses a single region of interest, based on the end-diastolic frame, to calculate the background-corrected time–activity curve. The LVEF calculated by this approach is usually about 5% lower than that obtained with the variable region of interest method. The method has the advantage of producing a smoother curve, which is more useful for calculating the filling and emptying rates.

The EF derived from background-corrected gated blood pool scan correlates well with that derived from contrast ventriculography (Bacharach *et al.*, 1979). The intra-observer variation in calculation of EF is about 3%, while the inter-observer variation is <5%. Similarly, calculation of right ventricular EF using a count-based method has been described (Maddahi *et al.*, 1979). However, the right atrial contribution to the right ventricular time–activity curve in the LAO view makes these data less reliable.

Ventricular volumes Left ventricular volumes can be calculated by either a geometric (area/length) method (Strauss *et al.*, 1979) or by a count-based method. The geometric method requires calibration of the gamma camera to determine the relative size of the left ventricle in each of two views in the image. The volume of the chamber is then calculated using either an area/length formula or the Simpson rule approach (to calculate the volume of irregularly shaped objects). A minimum error of about 20% can be expected with the geometric approach, due to operator variation in defining the borders of the chamber. The count-based method requires a blood sample as a counting standard and correction for attenuation of blood pool activity by overlying chest wall. The count-based method has better precision than the geometric approach (minimum error of about 10%) (Massie *et al.*, 1982), but may have substantial inaccuracy due to the difficulty of computing attenuation.

Quantification of regional wall motion can be achieved either by measuring regional radial shortening (Yasuda *et al.*, 1981; Tamaki *et al.*, 1986a) as in contrast angiography, or by calculation of regional EF (Maddox *et al.*, 1979). The digital nature of the data lends itself to the generation of functional images, such as EF images (Maddox *et al.*, 1978), paradox image (Holman *et al.*, 1979), and amplitude and phase images (Adam *et al.*, 1979; Links *et al.*, 1980) that can be used to characterize regional asynergy and asynchrony.

Phase analysis Functional images can reduce complex information to a single image representing both anatomy and physiology. The stroke